Surg Radiol Anat (2015) 37:731–741
DOI 10.1007/s00276-014-1409-0

REVIEW

Three-dimensional study of the skin/subcutaneous complex using in vivo whole body 3T MRI: review of the literature and confirmation of a generic pattern of organization

Christian Herlin · Alina Chica-Rosa · Gérard Subsol · Benjamin Gilles · Francesco Macri · Jean Paul Beregi · Guillaume Captier

Received: 13 March 2014 / Accepted: 18 December 2014 / Published online: 1 January 2015

Abstract
Purpose With a view to developing a tool for predicting the behavior of soft tissues during plastic surgery procedures, we looked for the existence of homologies in the overall pattern of organization of the skin/subcutaneous tissue complex between various body parts, using high-resolution in vivo imaging methods and data available in the literature.
Methods 3T MRI scanning sequences were performed using appropriate radiofrequency coils on the face, thorax, breast, abdomen and lower extremity of six healthy volunteers. The radiological findings were segmented and converted into volumetric data.
Results The superficial and deep adipose tissue was found to be clearly separated by an intermediate layer called stratum membranosum or superficial fascia. This continuous layer covered all the anatomical parts of the body examined. It was found to have several components in the trunk and limbs and to form a continuous layer with the superficial muscular aponeurotic system in the face. A retaining connective network consisting of superficial and deep retinacula cutis detected in all the regions investigated sometimes formed more densely packed structures playing the role of skin ligaments.
Conclusion The results of a 3T MRI study on subcutaneous tissue showed the existence of a common pattern of organization of the skin–subcutaneous tissue complex in the various parts of the body studied. This general model is subject to quantitative variations and tissue differentiation processes promoting the sliding or contractility of the supporting tissue. Three-dimensional reconstructions were obtained by post-processing the MRI images and will be used to perform pre-surgical simulations by settings a generic model that can be adapted to the different localization of the human body in a procedural way.

Keywords Skin · Soft tissues · Modeling · MRI · Superficial fascia · SMAS

C. Herlin · G. Captier
Department of Plastic and Craniofacial Pediatric Surgery, Hospital of Lapeyronie, University of Montpellier-Nîmes, 371 avenue du doyen Gaston Giraud, 34295 Montpellier, France

C. Herlin (✉)
Department of Plastic and Reconstructive Surgery, Wound Healing, Burns, Hospital of Lapeyronie, University of Montpellier-Nîmes, 371 avenue du doyen Gaston Giraud, 34295 Montpellier, France
e-mail: c-herlin@chu-montpellier.fr; christian.herl@free.fr; drchristianherlin@gmail.com

A. Chica-Rosa · F. Macri · J. P. Beregi
Department of Radiology, Hospital of Nîmes, University of Montpellier-Nîmes, Place du Pr Robert Debre, 30029 Nîmes, France

G. Subsol · B. Gilles
Laboratory of Informatics, Robotics and Microelectronics of Montpellier, CNRS/University of Montpellier, 161, rue Ada, 34090 Montpellier, France

G. Captier
Laboratory of Anatomy, University of Montpellier-Nîmes, 2, rue de l'Ecole de Médecine, 34000 Montpellier, France

Introduction

Surgeons [13, 14], biomechanists [21, 28] and digital designers are all looking for accurate and realistic means of predicting the behavior of soft tissues. Although different objectives have been pursued in each case, the main problem

has been that of modeling a heterogeneous three-dimensional structure showing complex mechanical behavior [10]. In fact, there exist no mechanical models so far which accurately simulate the anatomy of the skin/subcutaneous complex (SSC) formed by the tissues, taking the connective arrangements and the mobility of the components into account. The SSC includes the skin, the subcutaneous fat and connective means of union between the skin and the deep plane.

Most of the existing soft tissue models are uni- or bilamellar models in which the tissue thickness is taken to be constant and to show linear isotropic mechanical behavior. These models therefore differ considerably from the complex mechanical pattern of the human skin and adipose tissue, which are supported by the complex three-dimensional collagen network described in detail in many anatomical and histological studies [2, 26].

Although the structure of subcutaneous tissue differs between various regions of the human body, common components have been identified in several anatomical [1, 8] and radiological studies [6, 23, 24, 42]. The idea of developing a generic model for subcutaneous tissue which could be applied to various anatomical regions was first put forward 20 years ago by Lockwood [25], who presented a superficial fascial system (SFS) focusing on the trunk and limbs. Abu-Hijleh et al. [1] subsequently confirmed that the subcutaneous tissues show a similar pattern of distribution in the arms, legs and trunk. The anatomical descriptions available include one or several fibrous layers corresponding to the stratum membranosum (SM) usually called superficial fascia (SF) running parallel to the skin, which are crossed by fibrous septa called retinacula cutis (RC). On the surface of the SM and at deeper level, there also exist variable amounts of adipose tissue, known as superficial adipose tissue (SAT) and deep adipose tissue (DAT). Ferreira et al. [9] suggested the possibility of extending this stratigraphic model to include the face, in which case the superficial musculo-aponeurotic system (SMAS) was regarded as a specific version of the SFS.

The aims of this study were first to perform 3T MRI studies on the SSC in various body regions which are of particular interest in the field of plastic and reconstructive surgery, namely the face, the male chest and female breast, the abdomen, the lower limbs and the buttocks. The second goal was to determine how 3T MRI findings could help to draw up a generic three-dimensional geometrical model for the SSC.

Materials and methods

Three-dimensional data acquisition

Three-dimensional 3T MR imaging (GE HDXT 3T, General Electrics®, Minneapolis, USA) was performed under closely controlled physical conditions (temperature 25 °C, hygrometry 55 %).

Six healthy volunteers were selected for this purpose: three males and three females with age range between 21 and 52 years (Table 1). Two different signal weighting levels (T1 and T2) were used in the data acquisition procedure to study the adipose layers and the retaining connective network (RCN). The contrast was greater and the signal-to-noise ratio was lower with T2 than with T1. In the T1 relaxation kinetics, the differences between the signals decreased at a later stage and the contrast between the tissues was no longer sufficiently high. In addition, since the T1 contrast decreased, the artifacts induced by the movement, chemical shifts and the magnetic sensitivity increased in the 3T high field. The time elapsing between the two sequences was kept as short as possible and the volunteers were asked to remain motionless. The acquisition was carried out sequentially on the abdomen during apnea to prevent the occurrence of any artefacts. Four sequences, each consisting of 20 sections, were performed above and below the navel, taking care to keep the flexible radiofrequency coil consistently in the same position.

Details about the subjects and the MRI acquisition protocols are presented in Table 1.

Segmentation of the skin/subcutaneous tissue complex

Segmentation procedures were applied to DICOM images transferred to a special platform using the Myrian 1.15.1 software program (SAS Intrasense, Montpellier, France). With this program, multiplanar reconstruction procedures can be applied and regions of interest (ROI) attributed to anatomical structures [4, 15]. Images were segmented on the T2 spin echo acquisitions by using complementary information provided by visualizing the synchronized T1 images. In the case of structures like bones and fat, generating extreme signals, some thresholding algorithms provided with the software program were used. The other structures (muscles, fasciae, cartilage, aponeuroses, etc.) were segmented manually.

Several structures were identified to obtain a generic model of SSC: the skin, the superficial adipose tissue (SAT), the SM, consisting of the stratum fibrosum (SMAS) and the stratum musculosum (SMAS) distinguished in the face and the deep adipose tissue (DAT).

The underlying structures were segmented depending on their anatomical locations: the deep musculature surrounded by deep fasciae, the cartilage, bones (the skull, ribs, vertebrae, iliac bone, etc.), ligaments, eyes, parotid, mammary gland and blood vessels (without distinguishing between arteries and veins).

Table 1 Details of the subjects and the MRI acquisitions

	Subject no. 1		Subject no. 2	Subject no. 3		Subject no. 4	Subject no. 5		Subject no. 6	
Subjects' characteristics										
Age/sex	28/female		35/male	29/female		51/male	52/female		21/male	
Weight (kg)	52		78	54		86	69		67	
Height (m)	1.65		1.81	1.7		1.82	1.63		1.75	
Localization	Face		Breast	Thorax		Abdomen/lumbar region	Inferior limb		Buttocks	
Position	Supine		Prone	Supine		Supine	Supine		Supine	
Number of acquisitions	4 (subjects 1–4)		2 (subjects 2 and 5)	1 (subject 2)		1 (subject 3)	1 (subject 3)		1 (subject 3)	
Acquisition characteristics										
Weighting levels	T1	T2	T2	T1 (cardiac gating)	T2	T2	T1	T2	T1	T2
Radiofrequency coil	"Cranial" type with 32 channels		3 DT HD8CH vibrating breast coil with 8 channels	3 DT HD8CH torso array with 8 channels		3 DT HD8CH torso array with 8 channels	Standard		Standard	
Number of slices	420	395	80	142	125	4 × 20	3 × 128	3 × 128	128	128
Thickness of slices (mm)	1	1	2	2	2	1.5	2	2	2	2
Spacing (mm)	0.5	0.5	2	1	1	1	1	1	1	1

Some of the structures underlying the bones (the brain, lungs, deep muscles and pharynx) were not included in the model.

Results

The face

The skin could be clearly detected on all the sections. Its thickness ranged between 1 mm in the median part of the upper eyelids and 4 mm in the scalp and temporal region.

The SAT could be distinguished from the DAT because they were separated by one or two hyposignal layers (Fig. 1). The thickness of the SAT was found to be highly variable. It was indistinguishable at the level of the pre-tarsal orbicularis oculi muscle, the middle third of the nasal ridge and above the anterior part of the orbicularis oris muscle. The maximum thickness of the SAT (9 mm) was observed in the anterior and median parts of the pre-zygomatic adipose tissue.

The stratum membranosum was found to form a continuous layer running from the laterofacial part of the superior temporal line down to the lower edge of the body of the mandible. The galea capitis (epicranial aponeurosis) which continues cranially to the stratum membranosum plane was not viewed continuously mainly because the DAT was not visible above the superior temporal line. Below the lower edge of the mandible, this layer was contiguous with the platysma muscle ahead of the sterno-cleidomastoid muscle plan. It usually consisted of a single

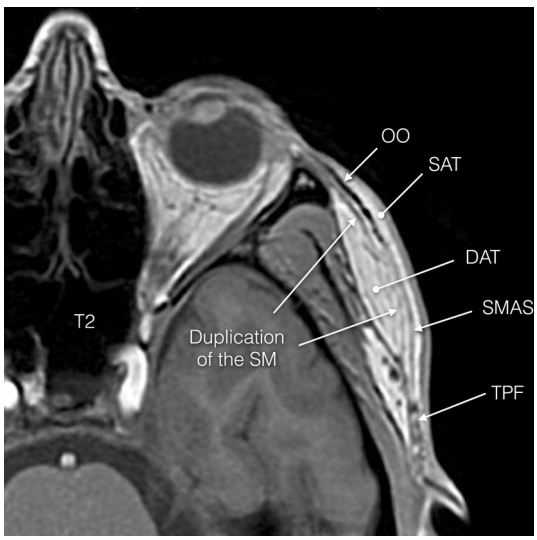

Fig. 1 MRI scan in axial plane of subject #1 at the level of the caudal temporal region showing the multi-stratigraphic pattern observed in the face. *OO* orbicularis oculi, *TPF* temporo-parietal fascia, *SAT* superficial adipose tissue, *DAT* deep adipose tissue, *SM* stratum membranosum, *SMAS* superficial musculo-aponeurotic system

hyposignal layer which was thicker anteriorly than laterally. In the temporal region, this plane corresponded to the temporoparietal fascia. Anteriorly, it formed a continuum with the plane of the orbicularis oculi muscle, and cranially it formed a continuum with the plane of the frontal belly of the occipitofrontalis muscle.

The trajectories of the main facial blood vessels (facial and temporal arteries and their main branches) often ran on the SM plane. In the zygomatic and temporal regions, the SM consisted of several layers (2–6). At the level of the postero-inferior quadrant of the temporal region, it was contiguous with the deep fascia of the temporalis muscle. On the axial plane, this continuous lamina extended over the whole of the face. It was thus easy to distinguish the SAT and the DAT, apart from the triangle formed by the summit of the nose and the two oral commissures. Inside this triangle, especially in the naso-jugal fold, the layers are intermingled, making the stratigraphic pattern more difficult to identify (Fig. 2).

Some of the muscles, such as the zygomaticus major muscle, the levator labii superioris alaeque nasi muscle, the risorius muscle and the medio-caudal part of the orbicularis oris muscle did not fit this stratigraphic pattern because their fibers crossed the DAT.

The breast and thorax

The average thoracic skin thickness was 3 mm. In the intermammary space, the stratigraphic pattern of the SM was less visible, since it merged medially with the pre-sternal plane. A more distinct pattern of stratification was observed cranially to the sternal manubrium and caudally to the submammary fold. The SM identified beyond the mammary region was continuous anteriorly, in the breast area, with a superficial hyposignal layer located 3–4 mm under the skin (corresponding to Patey's mastectomy plane). This plane was clearly interrupted at the level of the nipple. Posteriorly, a thin SM layer was sometimes visible, anteriorly from the pectoralis major muscle plane. It was often deduced from the change in the orientation of the perpendicular RCN (corresponding to the Cooper's ligament), which became oblique before merging with it. The Cooper's ligament sometimes seemed to interrupt the posterior duplication of the SM merging with the pectoralis major muscle fascia (Fig. 3).

A fairly similar pattern of organization was found to exist in the male thoracic region (Fig. 4). The RCN running perpendicular to the SM layers were less highly developed, and the superficial SM layer was less clearly visible than in the breast.

The back

We found mostly a single layer, which was thickened (Fig. 4). A clear apposition was visible along the spine.

The abdomen

The thickness of the skin was measured from 5 mm anteriorly to 7 mm into the lumbar region. In the antero-lateral part of the abdomen, the SM formed a single layer. More anteriorly, it divided into two parts when the adipose tissue

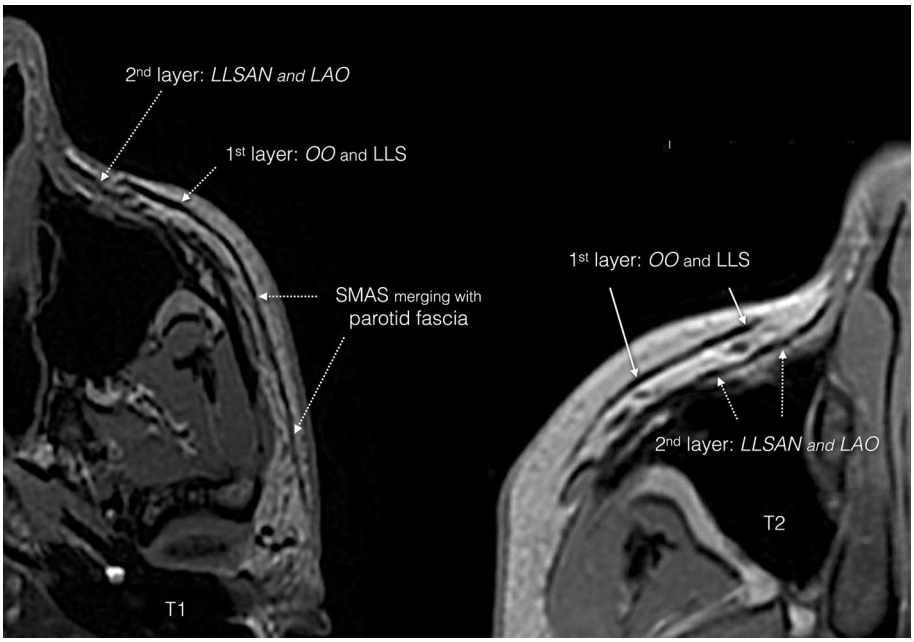

Fig. 2 MRI scan in axial plane at the level of the maxillary region highlighting the loss of the stratigraphic pattern medially to the naso-labial fold. *LLSAN* levator labii superioris alaeque nasi, *LAO* levator anguli oris, *LLS* levator labii superioris. On the *right* subject #3. On the *left* subject #2

Fig. 3 MRI scan in axial plane of subject #5 at the level of the areolar region focusing on the retaining connective network organization in the breast. The densification of the RCN constitutes the Cooper's ligament

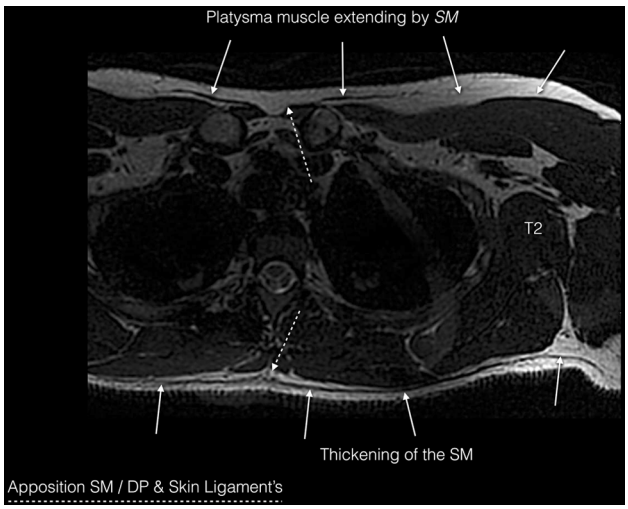

Fig. 4 MRI scan in axial plane of subject #2 at the level of the upper part of the thorax. Anteriorly, the platysma is in continuity with the SM. Posteriorly, the SM is found to be thickened. Laterally, the RCN density gradually increases

became thicker. In the peri-umbilical region, the SM took a deeper course and merged with the pre-muscular fasciae of the rectus abdominis muscles. In the posterior part, the SM was clearly detected in the middle of the subcutaneous tissue. This layer divided caudally, in the supra-gluteal region. Opposite the spinous processes, the SM merged with the premuscular fasciae of the erector spinal muscles before emerging again between the latter. Some regions were observed where the SM adhered to the posterior part of the fasciae of the external abdominal oblique muscle (Fig. 5).

The lower limbs and buttocks

The SM and RCN showed a similar pattern of organization in these areas to that described in the literature [2, 25, 27]. Indeed, the organization of SM seems quite similar at the level of all limbs (upper and inner) with one to two layers of SM found on the thighs and arms and one layer for the forearms and legs. The RCN is mostly undeveloped even among overweight people. It seems to be organized around the vascular and nervous elements.

However, that observed in the buttocks (Fig. 6) and knees (Fig. 7) was unusually heterogeneous. A clear-cut increasing gradient in the number of retinacula cutis was detected medially in the knee and buttocks, corresponding to the preferential fat storage sites.

Discussion

It is difficult to draw up a systematic description of the architecture of subcutaneous tissue: this problem is reflected in the lack of consensus between the terminology used in various countries, which has been pointed out by previous authors [1, 45, 47]. Nevertheless, most authors

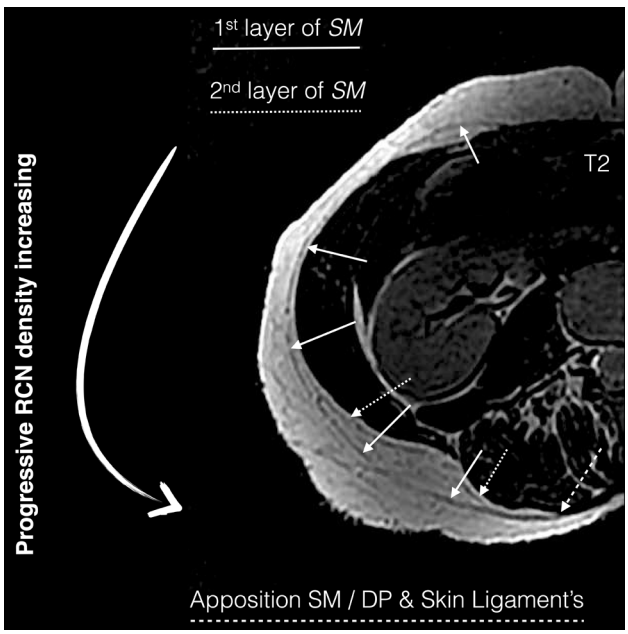

Fig. 5 Distribution of the retaining connective network at the level of the peri-umbilicus region (subject #1). The increase in thickness of the adipose tissue matches with a subsequent increase of the mesh formed by the RCN. Laterally and posteriorly, the RCN density gradually increases

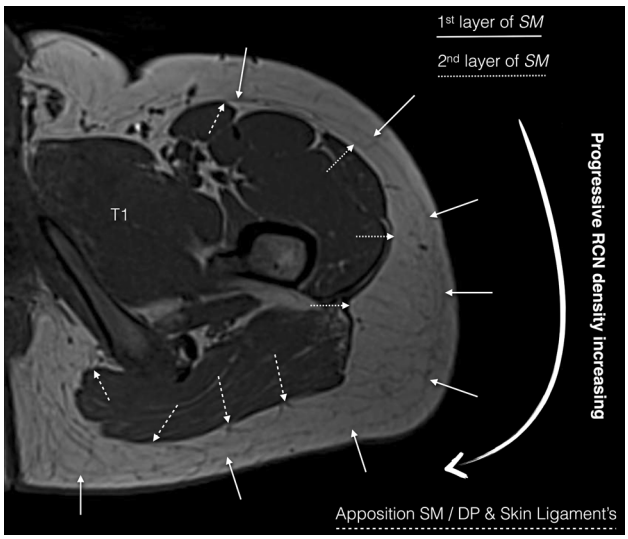

Fig. 6 Distribution of the retaining connective network at the level of the buttocks (subject #6). Laterally, the SM splits and then merges with a dense supporting network formed by RCN

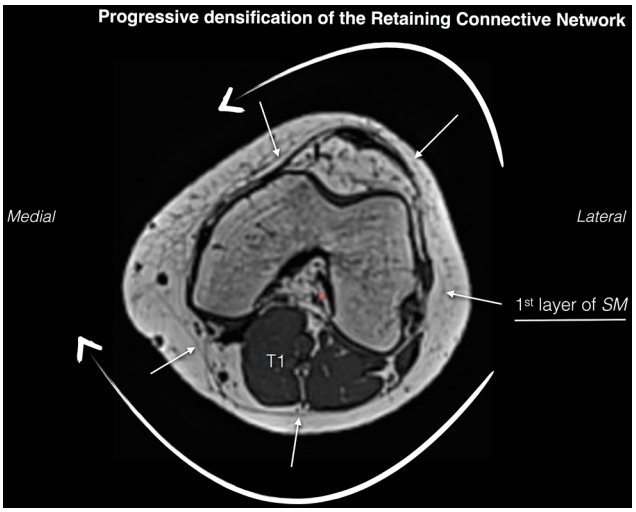

Fig. 7 Distribution of the retaining connective network at the level of the knee (subject #6). As in the region of the abdomen and buttocks, the increase in thickness of the adipose tissue is associated with an increase in the density of RCN

[23, 44, 45] have agreed that the subcutaneous tissues consist of three main components: the superficial adipose tissue (SAT), an intermediate membranous layer, the SM or superficial fascia which can be either fibrous and/or muscular and either single or multiple, and the deep adipose tissue (DAT).

Description of the retaining connective network in the skin/subcutaneous tissue complex

The biomechanical parameters of the SSC depend on the mechanical behavior of all the tissues (fat, collagen, elastin), its architecture, and especially on the relationships between the various layers (skin with SAT, DAT with deep level and skin with deep level). The SAT and DAT are crossed by dense fibrous septa called retinacula cutis superficialis (RCS) and retinacula cutis profondus (RCP). Inside this retaining connective network (RCN), the adipose tissue forms lobules separated by thin septa, as in a honeycomb. The structure and development of these retinacula cutis are indissociable from those of the fatty lobules. Whenever the thickness of the adipose panicle increases, these structures play a mechanical and physiological role, reinforcing the neighbouring adipocytes. They have been found to show considerable intra- and inter-individual variability [22, 31, 38].

As previously established in anatomical studies on the trunk and buttocks [23, 25, 27], the RCS are usually perpendicular to the skin and seem to play the role of perpendicular supports, whereas the RCP are more oblique, and tend to serve as parallel supports. This meshing system also seems to be involved in the dissipation of mechanical loads and in proprioceptive processes. The SM protects and sustains the major superficial veins [1, 3] by duplicating itself. This anatomy is characterized in ultrasound by an aspect of "Egyptian eye" mainly visible at the level of the limbs where the fatty layer is less developed. Duplications or densifications of the RCN promote also the passage of the perforating vessels and decreases their parietal tension.

From a surgical point of view, the SM became a dissection plane of reference for perforator flaps harvesting as the deep fascia is the good plane for fascio-cutaneous flaps [29, 36]. The sub-SM plane provides thinner flaps [19] with a thin subcutaneous layer that allows the skin to anchor tightly to the surface, avoiding the phenomenon of gliding sometimes criticized with fasciocutaneous flaps [17, 18].

The RCN, perpendicular to the skin, are stretched during the dissection of perforator flaps and allow some safety during harvesting. In case of propeller harvesting, the release of the RCN surrounding the vascular pedicle can prevent its strangulation during the twist.

Figure 8 presents an intraoperative picture of a thigh dermo-lipectomy performed after liposuction. This picture clearly shows the difference between the SM, the fat lobules, the RCP and the membranes of septa. Some lobules are full and others are emptied by liposuction. We can see clearly the densification of the fat lobule intersections called retinacula cutis (or skin ligaments in some particular regions).

From the mechanical point of view, the collagen fibers running perpendicular to the skin seem to serve contention purposes, whereas the layers running parallel to the skin, including the SM, tend to play a pressure resistance role [43].

In some anatomical regions, there also exist some direct skin attachments originating from the deep plane. These

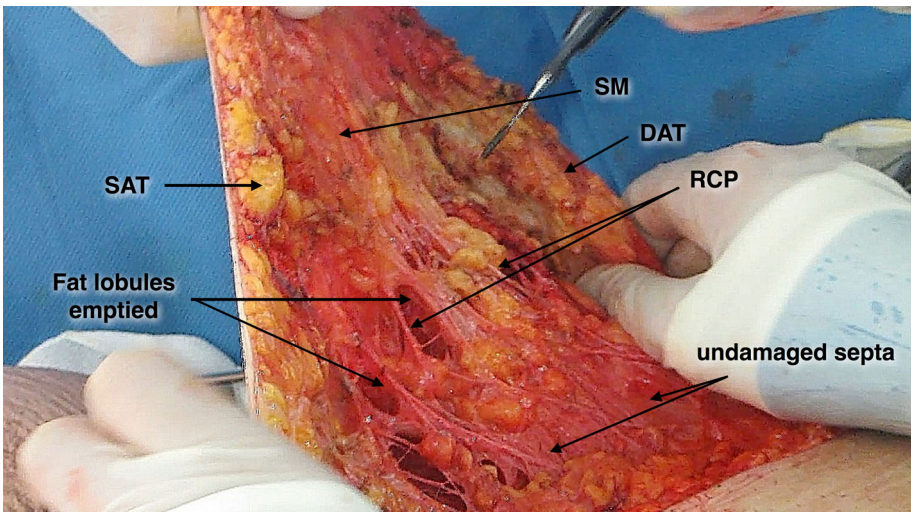

Fig. 8 Intraoperative view of a thigh dermo-lipectomy after liposuction. One can clearly distinguish the lobular structure of the SSC and the fibers of the RCP inserted at the deep level to the SM

connective components are usually called skin ligaments [33], in line with the Cooper's ligament [7] present in the breast and the Furnas' ligament [11] present in the face. Anchoring points have also been described at the abdominal and sternal levels by Lockwood [25], based on anatomical studies and the effects of excess body weight on the shape of the body. Some authors have previously described skin attachments of this kind in the fingers [48], the plantar sole [5], the palm of the hand and the scalp [1]. In our opinion, the term 'skin ligaments' should be used only to denote features involving the constant densification of the retinacula cutis whose topography is not dependent on the organization of fat lobules. In the present MRI study, we also established the existence in the abdomen and thorax of areas where the SM is in close contact with the deep tissue without any clearly visible vertical anchoring structures. At breast level, the collagen network running parallel to the galactophorous ducts showed a similar mechanical pattern of adhesion between the superficial and deep levels and can therefore be regarded as a densification of the RCP. These retaining structures have been studied particularly closely in the face with a view to understanding the effects of aging and improving existing methods of facial rejuvenation. Many attachment points have been described since the classical descriptions by McGregor and Furnas [11, 30, 46]. Since these structures differ in their density and the regions in which they are anchored, they have often been given different names (true ligaments, adhesions and septae) [2, 20, 30, 32]. These connective systems in the face subdivide the superficial and deep subcutaneous fat into compartments, which have been studied in detail by various authors, who reached fairly similar conclusions [34, 35, 39]. The compartmentation in question was described by Schaverien et al. [41] as a vascular delimitation corresponding to the boundaries of perforasomes [40]. In the present MRI study, the high spatial resolution made it possible to determine that the trajectory of the blood vessels indeed corresponded to the pattern of distribution of the RCN in the face, especially when they were crossing the DAT. Some perforating vessels running perpendicular to the cutaneous plane were sometimes found on the contrary to cross the SAT without showing any concomitant densification. In the thoracic, breast regions and the abdomen, a similar concordance between the emergence of perforating vessels and the pattern of distribution of the RCP was observed.

Integration of the face into the generic model

In the temporal and zygomatic regions, the SM was found to be divided into several layers. Abu-Hijleh et al. [1] previously described a similar pattern in the back, posterior forearms and thighs. This particular arrangement may contribute mechanically to stabilizing the superficial adipose layers. The presence of muscle fibers in the subcutaneous tissues of the face is a matter of controversy. The scattered relics of the panniculus carnosus present in other mammals undoubtedly also occur in humans (in the palmaris brevis, dartos, external anal sphincter and nipple subareolar muscle), but these features occur more systematically in the face muscles.

The idea that the SM and the SMAS may form a continuum has been previously put forward [9]. Although no anatomical evidence has been found for the existence of a continuum between the latero-facial SMAS, the temporo-parietal fascia, the centro-facial musculature and the platysma, many authors [9, 26, 30, 37, 44] have agreed that most of these muscles could be included in a single model, forming a musculo-aponeurotic hood around the face, separating the SAT from the DAT. In the present MRI

study, as in a study by Som et al. [42], considerable continuity was observed between the latero-facial SMAS, the temporoparietal fascia, the periorbital musculature and the platysma. At the centrofacial level, however, it was difficult to determine whether this line was continuous. The study by Gassner et al. [12] is consistent with our radiological findings on the loss of the stratigraphic pattern from the zygomaticus major muscle to the levator labii superioris alaeque nasi muscle. We observed the existence of a similar pattern in the risorius muscle. However, this regional specificity should be qualified by noting that the peribuccal (orbicularis oris) muscle is a particularly specialized and highly developed muscle.

Surgically, as described by many authors [12, 30], the releasing of main retaining ligaments is a key stage of facelifting ensuring redraping the skin and the SMAS in a higher position while reducing distortions and maintaining a stable result over time.

Advantages and limitations of 3T MRI for drawing up a generic model of the SSC

3T MRI provides a useful tool for identifying in vivo the structures constituting the SSC. Ultrasound methods have been successfully used to study some specific regions [1, 28, 45] and for the purpose of pathological analyses. However, these methods do not give a continuous three-dimensional picture of all the subcutaneous tissues in a single data acquisition. Tomodensitometric methods have also been used [6, 23, 27] to study the position of the SM in the abdomen. However, these methods are not suitable for studying more complex areas such as the face. They are suitable to studying the retinacula cutis and the connective components in areas where the neighbouring structures have similar levels of X-ray absorptivity. The use of 3T MRI was driven here by the need to optimize the spatial resolution. When dealing with the face and breasts, this method allows us to distinguish between the intermingled layers generating similar signals. This advantage was less relevant when dealing with larger areas, where the main problem was how to adjust the signal-to-noise ratio. The use of surface coils played an important role, but they had to be adapted from the standard settings. Abdomen image acquisition was performed sequentially on a patient in apnea, which prevented continuous volumetric acquisition but allowed us to obtain many details of the subcutaneous adipose structure. Homologies between the modes of stratification present in various body parts were brought to light by segmenting the images (Fig. 9).

Generic model of the skin–subcutaneous complex

From the architectural point of view, the conjunctive means of union supporting the skin and the SMAS along with the Cooper's and Furnas' ligaments and other deep points of attachment in the skin and the SM can be regarded as a densification of the RCN, as shown in the generic diagram of the SSC (Fig. 10). We think that the means of unions visible on MRI and on histological sections are most part of the time the sectional visualization of interlobular septa of the fatty layer and do not necessarily play a mechanical role. The skin ligaments should be considered as densifications or agglomerations of these septa, playing a major mechanical role in retaining the skin to the underlying tissue.

Likewise, the multi-stratified pattern described in many anatomical studies confers considerable generic architectural unity on the various structures running parallel to the superficial and deep layers (SM, Scarpa's fasciae, Colles' fasciae, SMAS, temporoparietal fasciae, preparotid fasciae, gallea, etc.).

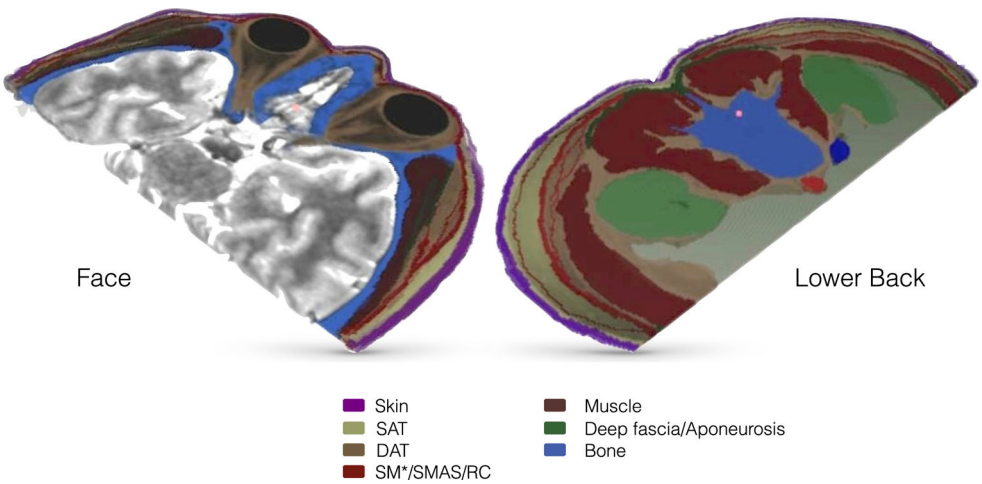

Fig. 9 Homologies between the patterns of distribution of the skin/subcutaneous tissue complex in the zygomatic and lumbar regions. In the places where the adipose tissue becomes thicker, the SM splits into two or more parts

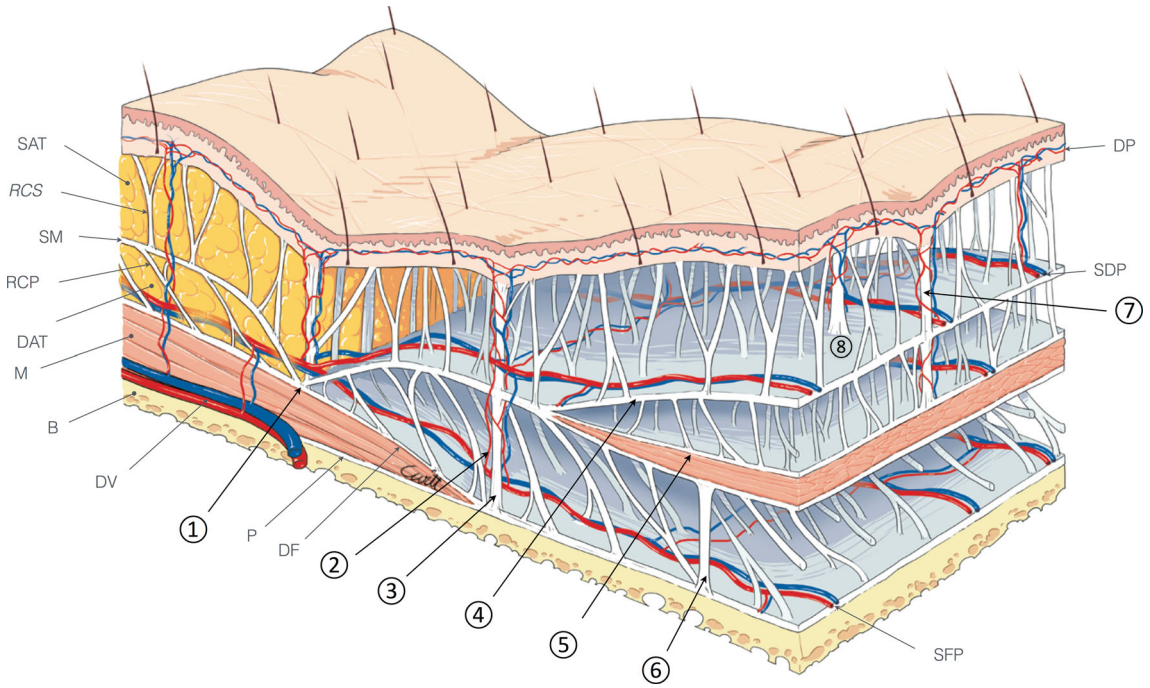

Fig. 10 Generic model of the skin/subcutaneous tissue complex. Depending on the regions, the SM adheres to the deep tissue and the SM splits into two parts. The RCS and RCP, densification of interlobular septae agglomerate to dense connective attachment between the various layers. The interlobular septa are not shown to allow a visual perspective. *SAT* superficial adipose tissue, *DAT* deep adipose tissue, *RCS* retinacula cutis superficialis, *RCP* retinacula cutis profondus, *M* muscle, *B* bone, *DV* deep vessels, *P* periosteum, *DF* deep fascia, *DP* dermal plexus, *SDP* sub-dermal plexus, *SFP* supra-fascial plexus. *1* Region of adhesion between the SM and the DP (opposite the sternum or the iliac crest). *2* Perforator's vessels running with RCP and RCS thickening. *3* "Skin ligaments" consisting of simultaneous densification of the RCS and RCP (Furnas' ligament, McGregor's patch, Cooper's ligaments). *4* SM duplication appearing mostly in fatty areas (cheeks, lower back, breasts, back, face posterior face of the arms, thighs, etc.). *5* Differentiation of the SM into muscle (cf: the SMAS, Dartos, nipple areolar muscle, corrugator cutis ani, palmaris brevis). *6* Thickening of the RCP connecting the SM and SMAS at a deep level. *7* and *8* Thickening of the RCSs connecting the SM and SMAS to the skin

Depending on their locations and functional specificities, some of the SM layers and the RCN were found to be subject to hypo- or hypertrophic differentiation tending to promote either tissue sliding, support or contractility. Based on the anatomical data available in the literature and the present findings, we have drawn up an overall stratigraphic model for the SSC including the sustaining connective network (Fig. 9), which seems to be applicable to all the parts of the body. This generic model will enable us to draw up several specific biomechanical models of the human SSC in various parts of the body by specifying the mechanical settings and the patient-specific architecture in a procedural way [16].

Conclusion

The multiplanar stratigraphic model of the subcutaneous tissue described in previous anatomical studies seems to be applicable everywhere in the human body. The few localizations where the morphological pattern observed does not correspond to this general model constitute only a tiny fraction of the whole body area. These occasional exceptions can be easily accounted for in terms of the under or overdevelopment of some layers.

In modeling studies, three-dimensional in vivo methods are necessary to obtain a realistic architectural picture. The 3T MRI images obtained here were processed to present the anatomical findings in the form of a geometrical model. This model will allow us to obtain patient-specific biomechanical models for predicting the behavior of soft tissues, which should be of great use in plastic surgery.

Acknowledgments The authors are grateful to the volunteers and the radiology technical team for their help in MRI acquisitions. They also thank Mrs Witt for the quality of the illustrations.

Conflict of interest The authors declare that they have no conflicts of interest. This study was not supported by any grants.

References

1. Abu-Hijleh MF, Roshier AL, Al-Shboul Q, Dharap AS, Harris PF (2006) The membranous layer of superficial fascia: evidence for its widespread distribution in the body. Surg Radiol Anat 6:606–619

2. Alghoul M, Codner MA (2013) Retaining ligaments of the face: review of anatomy and clinical applications. Aesthet Surg J 6:769–782
3. Caggiati A (2000) Fascial relations and structure of the tributaries of the saphenous veins. Surg Radiol Anat 3–4:191–196
4. Canovas F, Roussanne Y, Captier G, Bonnel F (2004) Study of carpal bone morphology and position in three dimensions by image analysis from computed tomography scans of the wrist. Surg Radiol Anat 3:186–190
5. Captier G, Fauré P, Chamoun M, Bonnel F (2003) Organisation anatomique et biomécanique de la sole plantaire. Med Chir Pied 19:9–12
6. Chopra J, Rani A, Rani A, Srivastava AK, Sharma PK (2011) Re-evaluation of superficial fascia of anterior abdominal wall: a computed tomographic study. Surg Radiol Anat 10:843–849
7. Cooper A (1840) On the Anatomy of the Breast. Longman
8. Dumont T, Simon E, Stricker M, Khan JL, Chassagne JF (2007) Analysis of the implications of the adipose tissue in facial morphology, from a review of the literature and dissections of 10 half-faces. Ann Chir Plast Esthet 3:196–205
9. Ferreira LM, Hochman B, Locali RF, Rosa-Oliveira LM (2006) A stratigraphic approach to the superficial musculoaponeurotic system and its anatomic correlation with the superficial fascia. Aesthet Plast Surg 5:549–552
10. Flynn C, Taberner AJ, Nielsen PM, Fels S (2013) Simulating the three-dimensional deformation of in vivo facial skin. J Mech Behav Biomed Mater 28:484–494
11. Furnas DW (1989) The retaining ligaments of the cheek. Plast Reconstr Surg 1:11–16
12. Gassner HG, Rafii A, Young A, Murakami C, Moe KS, Larrabee WF Jr (2008) Surgical anatomy of the face: implications for modern face-lift techniques. Arch Facial Plast Surg 1:9–19
13. Har-Shai Y, Bodner SR, Egozy-Golan D, Lindenbaum ES, Ben-Izhak O, Mitz V, Hirshowitz B (1996) Mechanical properties and microstructure of the superficial musculoaponeurotic system. Plast Reconstr Surg 1:59–70
14. Har-Shai Y, Sela E, Rubinstien I, Lindenbaum ES, Mitz V, Hirshowitz B (1998) Computerized morphometric quantitation of elastin and collagen in SMAS and facial skin and the possible role of fat cells in SMAS viscoelastic properties. Plast Reconstr Surg 7:2466–2470
15. Herlin C, Doucet JC, Bigorre M, Captier G (2013) Computer-assisted midface reconstruction in Treacher Collins syndrome part 2: soft tissue reconstruction. J Craniomaxillofac Surg 7:676–680
16. Herlin C, Gilles B, Subsol G, Captier G (2014) Generic 3D geometrical and mechanical modeling of the skin/subcutaneous complex by a procedural hybrid method. LNCS proceedings, ISBMS 2014 conference (in press)
17. Herlin C, Lievain L, Qassemyar Q, Michel G, Assaf N, Sinna R (2013) Freestyle free perforator flaps for heel reconstruction. Ann Chir Plast Esthet 4:283–289
18. Hong JP (2006) Reconstruction of the diabetic foot using the anterolateral thigh perforator flap. Plast Reconstr Surg 5:1599–1608
19. Hong JP, Yim JH, Malzone G, Lee KJ, Dashti T, Suh HS (2014) The thin gluteal artery perforator free flap to resurface the posterior aspect of the leg and foot. Plast Reconstr Surg 5:1184–1191
20. Knize DM (2007) The importance of the retaining ligamentous attachments of the forehead for selective eyebrow reshaping and forehead rejuvenation. Plast Reconstr Surg 3:1119–1120
21. Kuhlmann M, Fear EC, Ramirez-Serrano A, Federico S (2013) Mechanical model of the breast for the prediction of deformation during imaging. Med Eng Phys 4:470–478
22. Kumar P, Pandey AK, Kumar B, Aithal SK (2011) Anatomical study of superficial fascia and localized fat deposits of abdomen. Indian J Plast Surg 3:478–483
23. Lancerotto L, Stecco C, Macchi V, Porzionato A, Stecco A, De Caro R (2011) Layers of the abdominal wall: anatomical investigation of subcutaneous tissue and superficial fascia. Surg Radiol Anat 10:835–842
24. Li W, Ahn AC (2011) Subcutaneous fascial bands-a qualitative and morphometric analysis. PLoS ONE 9:e23987
25. Lockwood TE (1991) Superficial fascial system (SFS) of the trunk and extremities: a new concept. Plast Reconstr Surg 6:1009–1018
26. Macchi V, Tiengo C, Porzionato A, Stecco C, Vigato E, Parenti A, Azzena B, Weiglein A, Mazzoleni F, De Caro R (2010) Histotopographic study of the fibroadipose connective cheek system. Cells Tissues Organs 1:47–56
27. Markman B, Barton FE Jr (1987) Anatomy of the subcutaneous tissue of the trunk and lower extremity. Plast Reconstr Surg 2:248–254
28. Mazza E, Barbarino GG (2011) 3D mechanical modeling of facial soft tissue for surgery simulation. Facial Plast Surg Clin North Am 4:623–637
29. McGregor IA, Jackson IT (1972) The groin flap. Br J Plast Surg 1:3–16
30. Mendelson BC (2001) Surgery of the superficial musculoaponeurotic system: principles of release, vectors, and fixation. Plast Reconstr Surg 6:1545–1552
31. Mirrashed F, Sharp JC, Krause V, Morgan J, Tomanek B (2004) Pilot study of dermal and subcutaneous fat structures by MRI in individuals who differ in gender, BMI, and cellulite grading. Skin Res Technol 3:161–168
32. Moss CJ, Mendelson BC, Taylor GI (2000) Surgical anatomy of the ligamentous attachments in the temple and periorbital regions. Plast Reconstr Surg 4:1475–1490
33. Nash LG, Phillips MN, Nicholson H, Barnett R, Zhang M (2004) Skin ligaments: regional distribution and variation in morphology. Clin Anat 4:287–293
34. Pilsl U, Anderhuber F (2010) The chin and adjacent fat compartments. Dermatol Surg 2:214–218
35. Pilsl U, Anderhuber F, Rzany B (2012) Anatomy of the cheek: implications for soft tissue augmentation. Dermatol Surg 7:1254–1262
36. Ponten B (1981) The fasciocutaneous flap: its use in soft tissue defects of the lower leg. Br J Plast Surg 2:215–220
37. Prendergast PM (2012) Anatomy of the face and neck. In: Shiffman MA, Di Giuseppe A (eds) Cosmetic surgery. Springer, Berlin
38. Querleux B, Cornillon C, Jolivet O, Bittoun J (2002) Anatomy and physiology of subcutaneous adipose tissue by in vivo magnetic resonance imaging and spectroscopy: relationships with sex and presence of cellulite. Skin Res Technol 2:118–124
39. Rohrich RJ, Pessa JE (2007) The fat compartments of the face: anatomy and clinical implications for cosmetic surgery. Plast Reconstr Surg 7:2219–2227
40. Saint-Cyr M, Wong C, Schaverien M, Mojallal A, Rohrich RJ (2009) The perforasome theory: vascular anatomy and clinical implications. Plast Reconstr Surg 5:1529–1544
41. Schaverien MV, Pessa JE, Rohrich RJ (2009) Vascularized membranes determine the anatomical boundaries of the subcutaneous fat compartments. Plast Reconstr Surg 2:695–700
42. Som PM, Ann A, Stuchen C, Tang CT, Lawson W, Laitman JT (2012) The MR imaging identification of the facial muscles and the subcutaneous musculoaponeurotic system. Neurographics 2:35–43
43. Sommer G, Eder M, Kovacs L, Pathak H, Bonitz L, Mueller C, Regitnig P, Holzapfel GA (2013) Multiaxial mechanical properties and constitutive modeling of human adipose tissue: a basis for preoperative simulations in plastic and reconstructive surgery. Acta Biomater 11:9036–9048

44. Stecco C, Macchi V, Porzionato A, Duparc F, De Caro R (2011) The fascia: the forgotten structure. Ital J Anat Embryol 3:127–138
45. Stecco C, Tiengo C, Stecco A, Porzionato A, Macchi V, Stern R, De Caro R (2013) Fascia redefined: anatomical features and technical relevance in fascial flap surgery. Surg Radiol Anat 5:369–376
46. Stuzin JM, Baker TJ, Gordon HL (1992) The relationship of the superficial and deep facial fascias: relevance to rhytidectomy and aging. Plast Reconstr Surg 3:441–449
47. Wendell-Smith CP (1997) Fascia: an illustrative problem in international terminology. Surg Radiol Anat 5:273–277
48. Zwanenburg RL, Werker PM, McGrouther DA (2013) The anatomy and function of Cleland's ligaments. J Hand Surg Eur 5:482–484